PCCP

PAPER

Cite this: *Phys. Chem. Chem. Phys.*, 2018, **20**, 23747

Distribution of zwitter-ionic tryptophan between the micelles of 1-dodecyl-3-methyl imidazolium and aqueous medium from molecular dynamic simulation†

Elena A. Belyaeva, * Aleksandr A. Vanin and Alexey I. Victorov

Ionic liquids that form micelles have great potential as drug carriers and separating agents for bioactive substances. For such applications, a key issue is the distribution of the target substance between the micelle and its environment. We perform MD simulations to study solubilization of zwitter-ionic tryptophan in micelles of 1-dodecyl-3-methylimidazolium bromide. We found that the distribution of tryptophan depends strongly on the degree of counterion binding. A decrease in binding of bromide counterions leads to a substantial increase of the distribution coefficient. A dense layer of counterions at the micellar surface impedes the solubilization of the zwitter-ionic tryptophan but at the same time the presence of such a dense layer obstructs the washout of the solubilized tryptophan molecules from the micelle. Based on our simulation data, we conclude that an increase of the distribution coefficient of tryptophan between the micelle and water may be achieved by several means: by introducing counterions that bind weakly to the micelle (bulky ions whose charge is not strongly localized) and/or by employing micelle-forming ionic liquids with shorter alkyl chains to diminish the degree of counterion binding.

Received 18th April 2018,
Accepted 29th August 2018

DOI: 10.1039/c8cp02488j

rsc.li/pccp

Introduction

Alkyl substituted imidazolium salts carrying more than seven methylene units in the alkyl radical are known as surface-active ionic liquids (SAILs). A peculiar feature of this class of compounds is the combination of properties of an ionic liquid (IL) with those of a classical surfactant; SAILs form micelles in aqueous medium. Imidazolium-based SAILs often exhibit stronger surface activity than alkyl substituted quaternary ammonium salts.[1,2]

Micelles of cationic surfactants may solubilize a variety of substances, including proteins, nucleic acids, and drugs,[3] and act as carriers of chemotherapeutic agents.[4] The enhancement of a drug's solubility and targeting are challenging pharmaceutical issues. For delivery to tissues and organs, drugs must be sufficiently hydrophilic but they must be sufficiently lipophilic to travel across the cell membrane.[5] One of the ways to increase the solubility of drugs is to convert a sparingly soluble substance into its better soluble saline form: nearly 50% of all existing medicines are salts. Employment of solutions of ILs, particularly SAILs, not only helps to enhance the solubility of solid forms of drugs but also to administer their controlled delivery. One example of an enhancement of a drug's solubility with the aid of an IL is a 400–2000 fold increase of the solubility of glibenclamide (antidiabetic drug) upon addition of choline tryptophanate to an aqueous solution.[6] Controlled delivery of drugs with the aid of ILs and SAILs is also possible *via* introducing the drug in the cationic/anionic form in the IL or SAIL molecule. For example, the anti-inflammatory drug ibuprofen has been introduced in the form of the ibuprofenate anion in 1-alkyl-3-methyl-imidazolium ILs where alkyl is *n*-butyl, *n*-hexyl or *n*-octyl.[7] The presence of carboxylic groups in many drugs enables their efficient extraction and delivery using cationic micelles.[3,8]

Solubilization of aromatic substances in cationic micelles involves the electrostatic interactions between the electrons of a π-conjugated system and a SAIL's cations.[9–12] Solubilization of pyrene molecules in cetyltrimethylammonium bromide (CTAB) micelles has been studied by molecular dynamic (MD) simulation.[13] It has been shown that pyrene molecules are located in the palisade layer – an outer region of the alkyl core adjacent to the corona of the micelle. Owing to π–π conjugation, two pyrene molecules remain in parallel orientation for one third of the simulation time. Nevertheless the observed stacking had no significant effect on the overall micellar structure.

MD simulation has also been used to study solubilization of a pyrene + naphthalene mixture in sodium dodecylsulfate

Saint Petersburg State University 7-9, Universitetskaya Nab., St. Petersburg, 199034, Russia. E-mail: eabelyaeva@mail.ru

† Electronic supplementary information (ESI) available. See DOI: 10.1039/c8cp02488j

(SDS) micelles.[10] The results of simulations for varying concentration of naphthalene and pyrene show that additives have insignificant effect on the micellar structure. Most of the solubilized naphthalene and pyrene is located in the palisade layer within a distance of 1.5 nm from the center of mass of the micelle (COM). The solubilized naphthalene + pyrene mixture forms clusters of varying dimensions inside the micelle.[11]

Solubilization of four aromatic carbonic acids – phenylmethanoic acid (PhMA), phenylethanoic acid (PhEA), 3-phenylpropanoic acid (3-PhPA) and 3-phenylpropenoic acid (cinnamic acid, CA) – in CTAB micelles has been studied in ref. 14. Five, six, three and four solubilized molecules per micelle have been considered for PhEA, 3-PhPA, PhMA and CA, respectively. The acids do not penetrate deeper than in the palisade layer of the micelle in complete analogy with the behavior of other solubilization systems, as discussed above.

High biocompatibility of amino acids makes particularly important the development of techniques for their extraction and controlled delivery. An amino acid may exist in a neutral (zwitter-ionic), cationic or anionic form,[15] depending on the pH of the medium. Aromatic amino acids, *e.g.*, tyrosine, tryptophan (Trp) and phenylalanine associate in aqueous solutions owing to aromatic stacking, electrostatic and van der Waals interactions. A quantum-chemical study of proline–tryptophan complexes shows that T-shaped and stacked-like complexes are equally probable.[16,17] The latter are stabilized *via* π–π conjugation while the former are held by hydrogen bonds. In apolar solvents T-shaped complexes are energetically favorable because there are no competing H-bonds with the solvent. Stacked-like complexes predominate in polar solvents. In solutions of amphiphilic substances, for example in alcohols, both types of complexes are unstable.[16,17]

In this work we study solubilization of an essential hydrophobic amino acid,[18] tryptophan, in its zwitter-ionic form by a micelle of 1-dodecyl-3-methyl-imidazolium bromide [C_{12}mim]Br in aqueous solution. We examine the degree of extraction of tryptophan by the micelle from the medium, the arrangement of the solubilized molecules in the micelle, and association of tryptophan molecules in aqueous solution *vs.* that in the micelle.

Methods

Molecular-dynamic (MD) simulations have been performed using the isothermal–isobaric (*NPT*) ensemble with the aid of the GROMACS 4.6.5 software.[19] All-atom force fields have been used for the 1-dodecyl-3-methyl-imidazolium cation[20] and for tryptophan and bromide anions (Optimized Potential for Liquid Simulations, OPLS).[21] Simulation results for micelles of 1-dodecyl-3-methyl-imidazolium bromide in water with no added solubilizate have been reported previously.[22]

For nonelectrostatic interactions, we use the Lennard-Jones potential with the cutoff distance of 1.2 nm. The electrostatic interactions have been described by the Coulomb potential, using the Particle mesh Ewald method (with 1.2 nm cut-off).[23,24] Interactions between atoms separated by three or more bonds in the molecule are also described using the Lennard-Jones and Coulomb potentials. The constraints on bonds and angles have not been imposed. The Nose–Hoover thermostat[25] and the Parrinello–Rahman barostat[26] have been used to maintain constant temperature (298 K) and pressure (1 bar), respectively. For water molecules, we use the SPC/E (extended Simple Point Charge) model.[27] The approach of steepest descent was used for minimization of the energy in each system. Visualization of molecular trajectories has been performed with the VMD software.[28]

From electric conductivity experiments, the aggregation number of [C_{12}mim]Br is 43–67 (55 in average).[29–31] This is in good agreement with our previous MD simulations of a spherical micelle[22] at 0.2 M [C_{12}mim]Br in water. Our simulation shows no perceptible trend of the spherical aggregate for growth or shape transition; hence, our selected value of 55 for the aggregation number.

Initial configurations were prepared in three stages. The micelle [C_{12}mim]Br was placed in the periodic cell with the box side length of 8 nm (the structure of the micelle was obtained and investigated earlier[22]). Then, the required amount of tryptophan molecules was added to the box, and all free space of the periodic box was filled with water molecules. The tryptophan molecules were arranged in a random order, the micelle in the initial configuration did not contain any tryptophan molecules.

Significant changes in the systems occur during the first few nanoseconds. After the first nanosecond, the total energy reaches a steady-state value (since we work with the previously assembled micelles, significant structural rearrangements of the systems, accompanied by strong changes in the total energy, are not observed). Then a relaxation of the distribution of tryptophan molecules between the micelle and the environment takes place. This can be either a diffusion-limited process or a process that is limited by the direct crossing of the imaginary boundary between the micelle and the environment by a tryptophan molecule. In our case, we consider diffusion to be the main limiting factor. The reason can be well understood from the time dependence of the number of tryptophan molecules solubilized by a micelle. The instantaneous number of tryptophan molecules in a micelle changes constantly and very rapidly, oscillating about the mean value. The constancy of the length of the edges of the periodic cell, the constancy of the micelle's moment of inertia and the constancy of the number of tryptophan molecules solubilized in the micelle all served as equilibrium criteria. Each simulation run extended for no less than 40 ns with the time step of 2 fs. In the case of a diffusion-limited solubilization process, 10–20 nanoseconds are sufficient to achieve solubilization equilibrium.

Results and discussion

The concentration of tryptophan varied from 2.5×10^{-2} M to 1.6 M. Fig. 1 shows structures of Trp and [C_{12}mim]Br and the notation used for labeling of atoms.

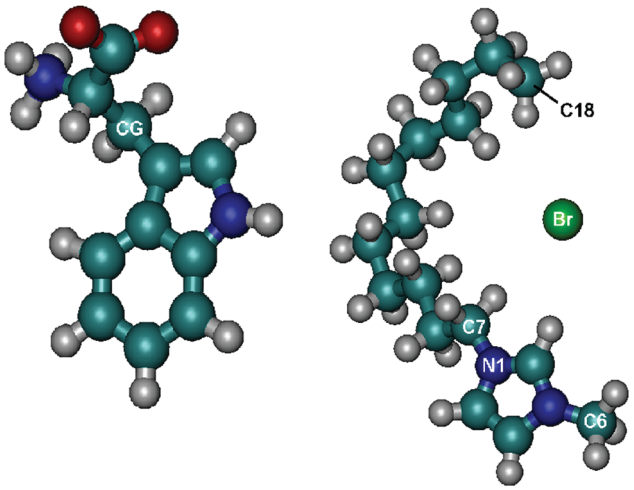

Fig. 1 Molecular structure and labeling of atoms for Trp (left) and [C_{12}mim]Br (right). Atoms are shown as color-coded spheres: oxygen – red, nitrogen – blue, carbon – cyan, hydrogen – grey, bromide anion – green.

Fig. 2a shows the local density profiles of different atoms in the [C_{12}mim]Br micelle, including Br^- counterions, oxygen atoms of water molecules, and atoms that belong to the head groups and tail groups of $[C_{12}mim]^+$ cations. The locations of the profile's maxima reflect local enrichment of the micelle in certain species. As reflected by the local densities of atoms C18 and C7, the palisade zone of the micelle extends up to 1.64 nm from the micelle's center of mass (COM). The local densities of atoms C7 and C6 show that micelle's corona stretches from 1.64 nm to 2.20 nm from COM. The major part of bromide ions resides within 1.80–2.10 nm from COM, in the micelle corona. Therefore the micellar radius may be estimated as 2.20 nm, corresponding to the location of the peak in the local density of C6 atoms. This local density falls off to zero at *ca.* 3.00 nm from COM. The outer part of the structure that stretches from 2.20 nm to 3.00 nm from COM is interpreted as the interface between the micelle and aqueous surroundings. Thus, based on our simulation data, we distinguish three principal parts in the micellar structure: the palisade, the corona and the interface. These principal parts are shown schematically in Fig. 2b. In our subsequent studies of solubilization, all the tryptophan molecules found closer than 3.00 nm off the COM in the equilibrated system have been qualified as solubilized by the micelle. The bromide ions have been considered bound to the micelle when located within the same distance from COM.

For each total concentration of tryptophan in the periodic cell, we obtained from the simulation data: the number of tryptophan molecules solubilized in the micelle, $N_{Trp}^{(m)}$; the number of tryptophan molecules in the aqueous surroundings of the micelle, $N_{Trp}^{(a)}$; the number of bromide anions bound and not bound by the micelle, $N_{Br}^{(m)}$, and $N_{Br}^{(a)}$, respectively.

The distribution coefficient of tryptophan, k, and the degree of binding of the bromide anions, α, have been calculated from

$$k = x_{Trp}^{(m)}/x_{Trp}^{(a)} \quad (1)$$

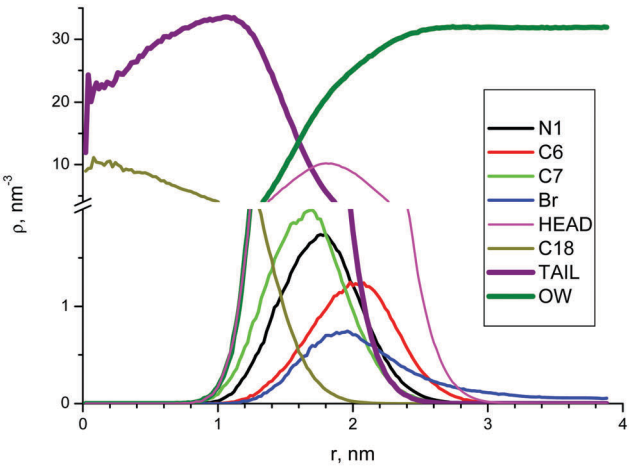

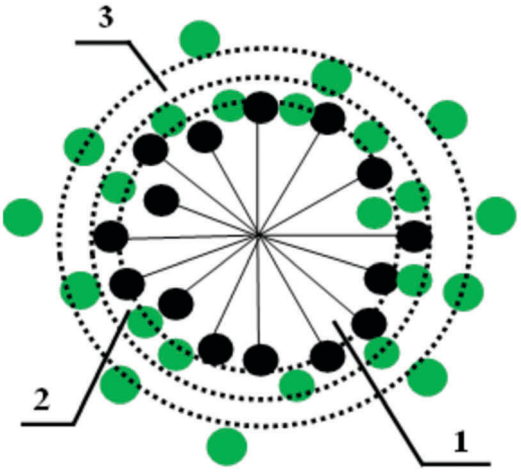

Fig. 2 (top) Local density profiles of atoms in the micelle [C_{12}mim]Br. Notation of atoms is shown in Fig. 1 (left), TAIL is the total local density for all carbon atoms of the hydrocarbon chain; r is the distance from the center of mass of the micelle. (bottom) Schematic of the micellar structure. The corona 2 ($1.64 \leq r \leq 2.20$ nm) accommodates the polar imidazolium rings; it separates the interface 3 ($2.20 \leq r \leq 3.00$ nm) between the micelle and aqueous surroundings (see text) from the palisade zone 1 ($r \leq 1.64$ nm) that contains the alkyl radicals; black circles – imidazolium rings, green circles – bromide ions, black lines – alkyl tails.

and

$$\alpha = N_{Br}^{(m)}/(N_{Br}^{(m)} + N_{Br}^{(a)}). \quad (2)$$

Here subscripts denote species (tryptophan molecules, bromide ions), superscripts (m) and (a) denote the micelle and the aqueous environment of the micelle, respectively; $x_{Trp}^{(m)}$ and $x_{Trp}^{(a)}$ are the mole fractions of tryptophan

$$x_{Trp} = \frac{N_{Trp}}{N_{Trp} + N_w + N_{Br} + N_{[C_{12}mim]}}, \quad (3)$$

where N_w, and $N_{[C_{12}mim]}$ are the numbers of water molecules and $[C_{12}mim]^+$ cations, respectively, either in the micelle (m), or in its aqueous environment (a).

Calculated results are given in Table 1. These results show that the distribution coefficient is essentially independent on

Table 1 Distribution of zwitter-ionic tryptophan molecules and bromide ions between [C_{12}mim]Br micelle and the surrounding aqueous solutions for varying total concentration of tryptophan in the system, C_{Trp}

C_{Trp}, M	$N_{Br}^{(m)}$	α, %	$N_{Trp}^{(m)}$	$N_{Trp}^{(a)}$	k
0.025	36	65	1.1	6.9×10	0.71
0.05	36	66	2.3	1.4×10^1	0.70
0.1	36	65	5.2	2.7×10^1	0.84
0.2	35	63	9.2	5.5×10^1	0.71
0.4	33	59	23	1.0×10^2	0.92
0.8	32	58	40	2.2×10^2	0.70
1.4	34	61	76	3.7×10^2	0.71
1.6	32	58	88	4.2×10^2	0.75

the concentration of tryptophan within a wide concentration range. The average distribution coefficient is 0.76 ± 0.09. The degree of binding of bromide ions is *ca.* 62%.

Fig. 3 shows a linear dependence between the number of solubilized molecules and the number of tryptophan molecules in the aqueous environment of the micelle. For different total concentrations of tryptophan in the system, the number of tryptophan molecules in solution around the micelle exceeds, approximately five times, the number of solubilized tryptophan molecules.

Structural details of a micelle containing tryptophan molecules may be inferred from Fig. 4. There is no substantial change in the micellar structure relative to a pure [C_{12}mim]Br micelle that does not contain solubilized molecules, *cf.* Fig. 2a. MD simulation of the system (at 40 ns run) that contains the [C_{12}mim]Br micelle, tryptophan and water shows that neither the shape nor the size of the micelle undergoes appreciable change: the palisade is within 1.64 nm from COM, the corona is in the interval 1.64–2.20 nm, the interface between micelle and the aqueous surroundings stretches from 2.20 nm to 3.00 nm and the major part of bromide ions is located within 1.74–2.20 nm from COM. These parameters are very close to those obtained for the [C_{12}mim]Br micelle in water with no added tryptophan (Fig. 2a).

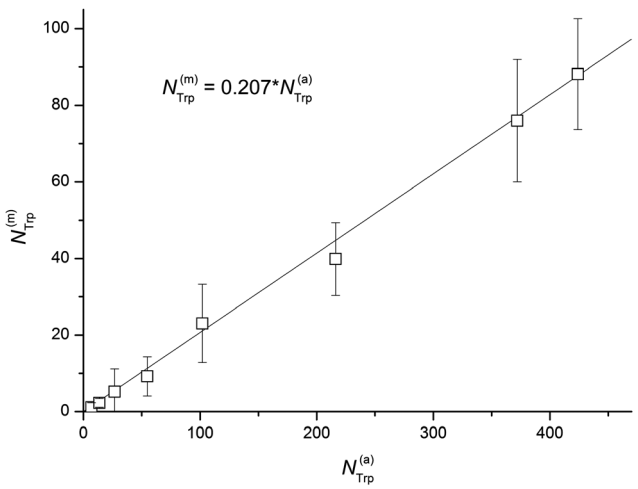

Fig. 3 The number of solubilized tryptophan molecules *vs.* the number of tryptophan molecules in the aqueous solution around a single [C_{12}mim]Br micelle. Shown are 3σ-error bars.

Most of the solubilized tryptophan molecules reside within the distance 2.20–3.00 nm from COM. Up to 1% of tryptophan molecules are localized in the palisade, 5% are in the corona, 14% are at the interface between micelle and the aqueous surroundings, while 80% of tryptophan molecules are outside the micelle beyond 3.00 nm from COM (Fig. 4). Thus only 20% of the total amount of zwitter-ionic Trp is solubilized by the micelle of [C_{12}mim]Br. A different picture is observed for systems at high tryptophan content: for 1.6 M total tryptophan, the micellar structure becomes somewhat loose. A less compact structure of the micelle's corona reflected by partial smearing of the local profiles shown in Fig. 4d, is a signature of an upcoming micelle breakup. The complete disaggregation process may require prohibitively long simulation times (hundreds of nanoseconds), however we did observe a substantial change of the aggregate's shape and the reduction of the aggregation number (the micelle has lost six monomers in 60 ns) that manifest pre-transition into the state of singly dispersed molecules.

Our results agree with those from the previous work on the solubilization of neutral tryptophan in the micelle of hexadecyltrimethylammonium bromide (HTAB):[32] tryptophan molecules are solubilized in the outer part of the palisade, in the micelle's corona and at the interface between micelle and the aqueous surroundings.

To reach the micelle interior the tryptophan molecule has to pass through the layer of counterions bound to the micelle. The degree of anion binding to the micelle is fairly high (58–66%, see Table 1). We examined the effect of the density of the counterion's layer on the uptake of tryptophan. Simulations have been performed for micelles having a lower degree of binding of bromide ions than those in Table 1, see Table 2. Three cations and a portion of bromide ions have been removed from the system that contains 32 tryptophan molecules and a [C_{12}mim]Br micelle with aggregation number 55 in water. These newly prepared systems were simulated for 40 ns. Our MD-data show that the dense layer of counterions around the micelle hinders the transfer of the tryptophan molecules in the interior of the micelle. For the degree of anion binding to the micelle of 49%, the obtained values of the distribution coefficient (0.78 ± 0.16) do not essentially differ from those given in Table 1. Further decrease in the degree of binding down to 37% and 19% gives the distribution coefficient 1.6 ± 0.4 and 1.1 ± 0.6, respectively. Thus, a decrease in the degree of anion binding to the micelle promotes penetration of tryptophan molecules inside the micelle leading to an increase of the distribution coefficient (by factor of 1.5–2.0 in our simulations).

To study the effect of the counterion layer on the tryptophan molecules that have already been solubilized in the micelle, a micellar aggregate containing 27 solubilized tryptophan molecules has been inserted in pure water. Upon simulating the system for 40 ns, from 3 to 8 tryptophan molecules (out of a total 27) were found within 3.00 nm from the micelle's COM. The degree of binding of bromide counterions increased from the initial 59% up to 68%. The distribution coefficient of tryptophan between the micelle and the aqueous environment is 1.1 ± 0.4. For this system, the number of bound bromide ions

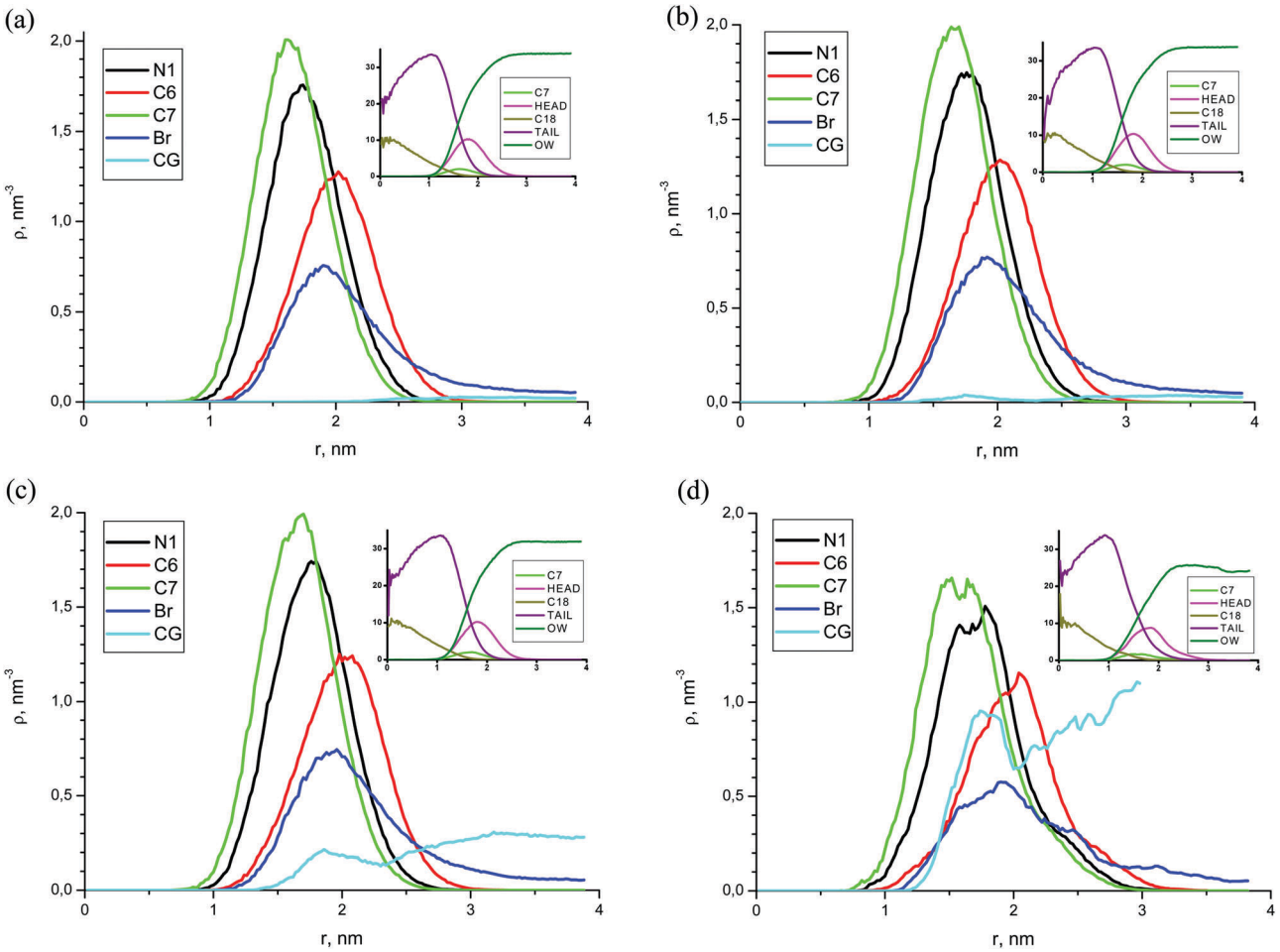

Fig. 4 The effect of tryptophan total concentration on the profiles of local density for atoms in the head groups (C6, N1, C7) and tail groups of $[C_{12}mim]^+$ (TAIL is the total local density for all carbon atoms of the hydrocarbon chain, C18 is the terminal carbon atom), counterions (Br), tryptophan (CG), and oxygen in water (OW). $C_{Trp} = 2.5 \times 10^{-2}$ M (a), 0.05 (b), 0.4 (c), 1.6 (d).

Table 2 Compositions of simulated systems with a diminished degree of counterion binding

	$N_{[C12mim]}$	N_{Br}	N_{Trp}	k	α, %
System 1	52	33	32	0.78	49
System 2	52	22	32	1.58	37
System 3	52	11	32	1.09	19

is somewhat larger than for the systems of Table 1. Bromide ions and tryptophan are likely to form a layer where they hold together, opposing the washout of one another from the micelle.

We thus may conclude that the layer of counterions has a substantial impact on the parameters of tryptophan solubilization. On the one hand the interaction with this layer and steric hindrance impede the penetration of tryptophan molecules in the micelle but on the other hand and for the same reasons this layer also obstructs the washout of the solubilized tryptophan molecules from the micelle.

Because simulation of each system has been performed, on average, for 60–80 ns, it is in principle possible that solubilized tryptophan molecules had not enough time to reach deeper inside the micelle. To check this possibility we performed a series of simulations where a molecule of tryptophan has been initially placed at different distances from COM (0.4–3.0 nm). Simulated systems contain one tryptophan molecule in the micelle of the aggregation number 55, see Fig. 5.

The tryptophan molecule initially located within the layer of counterions (1.8–2.1 nm from COM) diffuses within the micellar corona in the course of simulation while the molecule initially placed closer to COM enters the corona or the interface and remains there. This result confirms that the preferential accommodation of solubilized tryptophan is in the micellar corona or in the interface. The tryptophan molecule that has initially been placed outside the micelle, remains in solution, Fig. 5. We may also conclude that the crucial contribution to the interaction between the micelle and the solubilized tryptophan comes from interactions of tryptophan molecules with the imidazolium rings and with the adjacent methylene groups of 1-dodecyl-3-methylimidazolium. These interactions include the electrostatic, hydrophobic and aromatic contributions. The electrostatic contribution comes from interactions of charges on the tryptophan molecule with 1-dodecyl-3-methylimidazolium

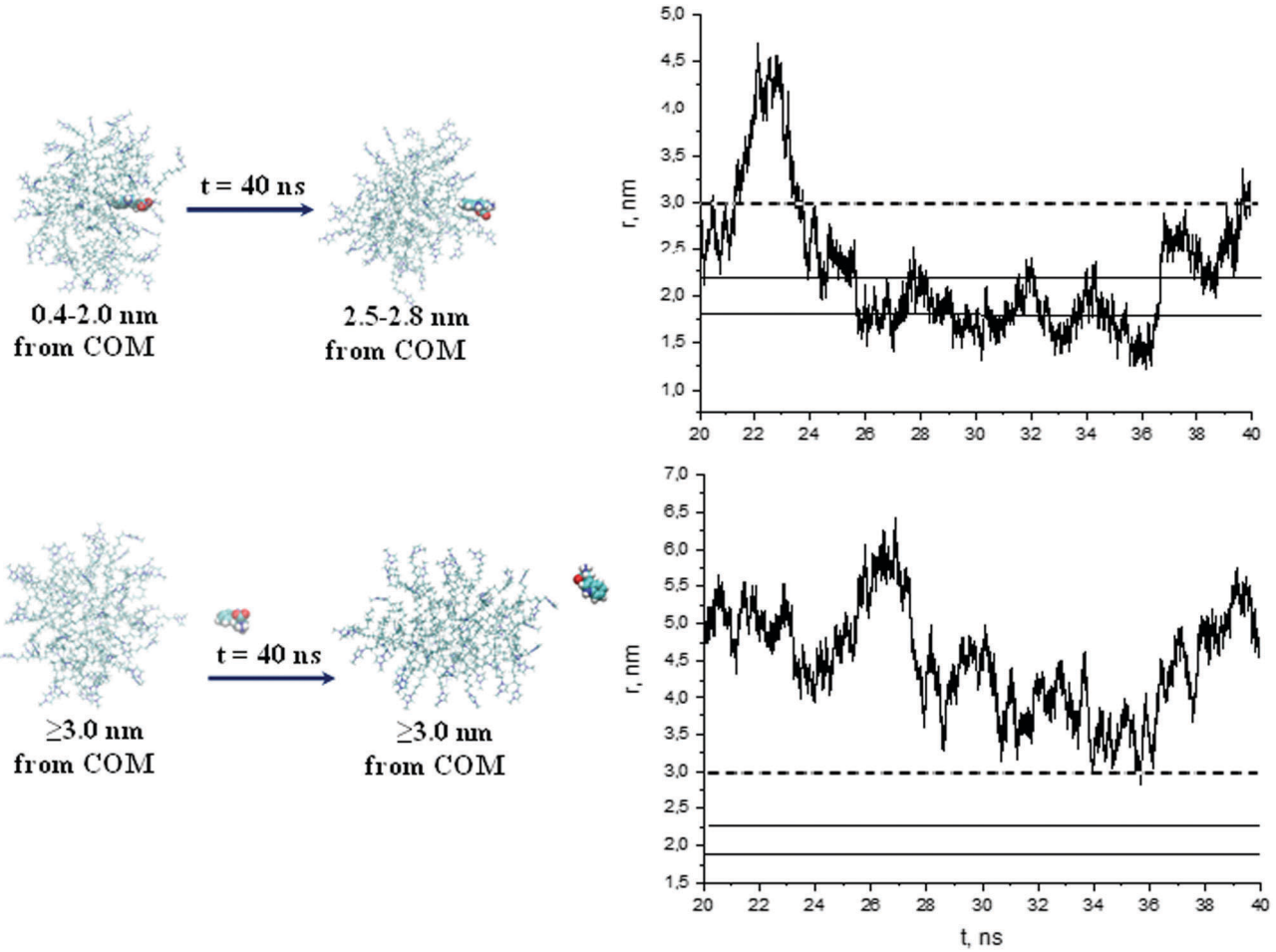

Fig. 5 Change of location of a tryptophan molecule after 40 ns MD-simulation runs.

cations of the micelle, with the bromide anions in the counter-ion layer, and with charges on other tryptophan molecules. Aromatic interaction between the imidazolium and tryptophan rings requires parallel orientation of these rings. Inside the micelle, the neutral tryptophan molecule may take suitable orientations, resulting in aromatic stacking with imidazolium.

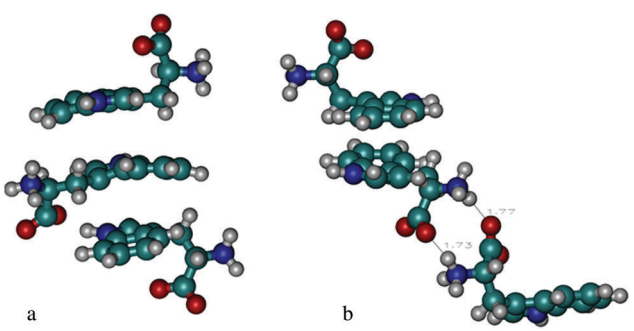

Fig. 6 Trimeric associates of tryptophan molecules. (a) A stacked-like trimer with π–π- bonds (with length ~ 3.7 Å) formed between the planar indole rings; (b) a mixed trimer with a π–π-bond and two ionic bonds between the oxygens of carboxyl groups and the hydrogens of ammonium cations (bond lengths are shown in Angstroms).

Tryptophan molecules may associate inside the micelle and in the aqueous medium. For a total concentration of tryptophan up to 0.2 M, the clusters are preferentially formed *via* interaction between the zwitter-ionic groups of amino acids (Fig. 6b), stacked-like complexes (Fig. 6a) have been observed more rarely, both in water and in the micelle. Such complexes start to dominate with an increase of tryptophan concentration and may include up to 5–7 tryptophan molecules. Free tryptophan molecules interact with those solubilized by the micelle and form the second layer of solubilized molecules.

Conclusions

The distribution coefficient of zwitter-ionic tryptophan between the micelle of 1-dodecyl-3-methylimidazolium bromide and an aqueous solution does not depend on the tryptophan concentration in the system: its value is 0.76 ± 0.09 in the concentration interval 0.025–1.6 M total tryptophan. The degree of binding of bromide ions to the micelle is 58–66%. For 1.6 M and higher total concentration of tryptophan, the micellar structure becomes somewhat loose. For lower tryptophan concentration, the micellar structure is nearly identical to that of a micelle in

pure water.[22] A decrease in the degree of anion binding to the micelle down to 25–30% of the total number of bromide counterions leads to an increase of the tryptophan distribution coefficient by a factor of 1.5–2.

Solubilized tryptophan molecules accommodate preferentially in the micellar corona and in the interface between the micelle and its aqueous surroundings. A substantial part of tryptophan molecules associate; at a total tryptophan concentration 0.2 M and higher the majority of tryptophan molecules form stacked-like complexes.

Interestingly, the presence of a dense layer of counterions at the micellar surface impedes the solubilization of tryptophan on the one hand but on the other hand the presence of such a dense layer also obstructs the washout of the solubilized tryptophan from the micelle.

The distribution coefficient of tryptophan between the micelle of 1-dodecyl-3-methylimidazolium bromide and its aqueous surroundings may be increased by several means: by introducing counterions weakly binding to the micelle (bulky ions whose charge is not strongly localized) and/or by employing micelle-forming ILs with shorter alkyl chains; it is known that for such micelles, the degree of anion binding to the micelle diminishes.[29]

Conflicts of interest

There are no conflicts of interest to declare.

Acknowledgements

We thank the Russian Science Foundation (project # 16-13-10042) for financial support, the resource center ''Computer center'' of Saint Petersburg State University and Moscow State University supercomputer center (''Lomonosov'' supercomputer) for the access to high-performance computers.

References

1 A. Bhadani, T. Misono, S. Singh, K. Sakai, H. Sakai and M. Abe, *Adv. Colloid Interface Sci.*, 2016, **231**, 36–58.
2 Z. H. Song, X. Xin, J. L. Shen, J. M. Jiao, C. X. Xia, S. B. Wang and Y. Z. Yang, *Colloids Surf., A*, 2017, **518**, 7–14.
3 L. Casal-Dujat, P. C. Griffiths, C. Rodriguez-Abreu, C. Solans, S. Rogers and L. Perez-Garcia, *J. Mater. Chem. B*, 2013, **1**, 4963–4971.
4 S. Qamar, P. Brown, S. Ferguson, R. A. Khan, B. Ismail, A. R. Khan, M. Sayed and A. M. Khan, *J. Colloid Interface Sci.*, 2016, **481**, 117–124.
5 D. J. Smith, J. K. Shah and E. J. Maginn, *Mol. Pharmacol.*, 2015, **12**, 1893–1901.
6 M. A. Alawi, I. I. Harridan, A. A. Sallam and N. Abu Heshmeh, *J. Mol. Liq.*, 2015, **212**, 629–634.
7 C. Tourne-Peteilh, B. Coasne, M. In, D. Brevet, J. M. Devoisselle, A. Vioux and L. Viau, *Langmuir*, 2014, **30**, 1229–1238.
8 W. L. Hough, M. Smiglak, H. Rodriguez, R. P. Swatloski, S. K. Spear, D. T. Daly, J. Pernak, J. E. Grisel, R. D. Carliss, M. D. Soutullo, J. H. Davis and R. D. Rogers, *New J. Chem.*, 2007, **31**, 1429–1436.
9 R. Masrat, M. Maswal and A. A. Dar, *J. Hazard. Mater.*, 2013, **244**, 662–670.
10 X. J. Liang, M. Marchi, C. L. Guo, Z. Dang and S. Abel, *Langmuir*, 2016, **32**, 3645–3654.
11 P. A. Bhat, G. M. Rather and A. A. Dar, *J. Phys. Chem. B*, 2009, **113**, 997–1006.
12 A. A. Dar, G. M. Rather and A. R. Das, *J. Phys. Chem. B*, 2007, **111**, 3122–3132.
13 F. F. Gao, H. Yan and S. L. Yuan, *Mol. Simul.*, 2013, **39**, 1042–1051.
14 S. S. Shah, K. Naeem, S. W. H. Shah and H. Hussain, *Colloids Surf., A*, 1999, **148**, 299–304.
15 A. Benedetto and P. Ballone, *Philos. Mag.*, 2016, **96**, 870–894.
16 F. L. Gervasio, R. Chelli, M. Marchi, P. Procacci and V. Schettino, *J. Phys. Chem. B*, 2001, **105**, 7835–7846.
17 R. Chelli, F. L. Gervasio, P. Procacci and V. Schettino, *J. Am. Chem. Soc.*, 2002, **124**, 6133–6143.
18 A. Ellington and J. M. Cherry, *Current Protocols in Molecular Biology*, John Wiley & Sons, Inc., 2001, DOI: 10.1002/0471142727.mba01cs33.
19 B. Hess, C. Kutzner, D. van der Spoel and E. Lindahl, *J. Chem. Theory Comput.*, 2008, **4**, 435–447.
20 C. Cadena and E. J. Maginn, *J. Phys. Chem. B*, 2006, **110**, 18026–18039.
21 W. L. Jorgensen, D. S. Maxwell and J. TiradoRives, *J. Am. Chem. Soc.*, 1996, **118**, 11225–11236.
22 E. A. Belyaeva, A. A. Vanin, Y. A. Anufrikov and N. A. Smirnova, *Colloids Surf., A*, 2016, **508**, 93–100.
23 T. Darden, D. York and L. Pedersen, *J. Chem. Phys.*, 1993, **98**, 10089–10092.
24 U. Essmann, L. Perera, M. L. Berkowitz, T. Darden, H. Lee and L. G. Pedersen, *J. Chem. Phys.*, 1995, **103**, 8577–8593.
25 P. Procacci, T. Darden and M. Marchi, *J. Phys. Chem.*, 1996, **100**, 10464–10468.
26 M. Parrinello and A. Rahman, *J. Appl. Phys.*, 1981, **52**, 7182–7190.
27 H. J. C. Berendsen, J. R. Grigera and T. P. Straatsma, *J. Phys. Chem.*, 1987, **91**, 6269–6271.
28 W. Humphrey, A. Dalke and K. Schulten, *J. Mol. Graphics*, 1996, **14**, 33–38.
29 T. Inoue, H. Ebina, B. Dong and L. Q. Zheng, *J. Colloid Interface Sci.*, 2007, **314**, 236–241.
30 R. Vanyur, L. Biczok and Z. Miskolczy, *Colloids Surf., A*, 2007, **299**, 256–261.
31 J. Wang, L. Zhang, H. Wang and C. Wu, *J. Phys. Chem. B*, 2011, **115**, 4955–4962.
32 A. Mukhija and N. Kishore, *Colloids Surf., A*, 2017, **513**, 204–214.